Available online at www.sciencedirect.com

ScienceDirect

Procedia Computer Science 76 (2015) 47 – 52

Procedia Computer Science

2015 IEEE International Symposium on Robotics and Intelligent Sensors (IRIS 2015)

Non-Contact Dual Pulse Doppler System Based Real-Time Relative Demodulation and Respiratory & Heart Rates Estimations for Chronic Heart Failure Patients

Vinh Phuc Tran[a,b,]*, Adel Ali Al-Jumaily[a]

[a]*Centre for Health Technologies, Faculty of Engineering & IT, University of Technology, Sydney, 15 Broadway, Ultimo NSW 2007, Australia*
[b]*Healthcare Informatics, ResMed Ltd., 1 Elizabeth Macarthur Drive, Bella Vista NSW 2153, Australia*

Abstract

Long-term continuous patient monitoring is required in many health systems for monitoring and analytical diagnosing purposes. Most of monitoring systems have shortcomings related to their functionality and/or patient comfortably. Non-contact monitoring systems have been developed to address some of these shortcomings. One of such systems is non-contact physiological vital signs assessments for chronic heart failure (CHF) patients. This paper presents novel real-time demodulation technique and estimations algorithms for the non-contact physiological vital signs assessments for CHF patients based on a patented novel non-contact bio-motion sensor. A database consists of twenty CHF patients with New York Heart Association (NYHA) Heart Failure Classification Class II & III, whose underwent full Polysomnography (PSG) analysis for the diagnosis of sleep apnea, disordered sleep, or both, were selected for the study. The propose algorithms analyze the non-contact bio-motion signals and estimate the patient's respiratory and heart rates. The outputs of the algorithms are compared with gold-standard PSG recordings. Across all twenty CHF patients' recordings, the respiratory rate estimation median accuracy achieved 91.52% with median error of ±1.31 breaths per minute. The heart rate estimation median accuracy achieved 91.29% with median error of ±6.16 beats per minute. A potential application would be home continuous sleep and circadian rhythm monitoring.

Peer-review under responsibility of organizing committee of the 2015 IEEE International Symposium on Robotics and Intelligent Sensors (IRIS 2015)

Keywords: non-contact Doppler radar; bio-motion signal processing; non-contact vital signs estimation;

* Corresponding author.
E-mail address: Vinh.P.Tran-1@student.uts.edu.au

Peer-review under responsibility of organizing committee of the 2015 IEEE International Symposium on Robotics and Intelligent Sensors (IRIS 2015)
doi:10.1016/j.procs.2015.12.274

1. Introduction

Obstructive sleep apnea (OSA) is a common and potentially lethal sleep disorder affecting 10 – 17% for males and 3 – 9% for females in the United States of America [1]. OSA is the cessation of airflow due to the collapse of the upper airway during sleep and can occur at any age, from infancy to old age. Research evidences have indicated that OSA is associated with ischemic heart disease, increased prevalence of stroke, coronary artery disease, atrial fibrillation, chronic heart failure (CHF) and cardiac sudden death [2]. Non-contact Doppler radar systems have been researched for the detection of physiological motions since 1970's. The majorities of the published results to date have been focused on the estimations of physiological rates, such as, respiratory and heart rates for both healthy and sleep disordered breathing (SDB) subjects. However, the sleep application of non-contact physiological vital signs assessments for CHF patients has been limited. It is also important to emphasize that the majorities of current reported achievements for non-contact physiological vital signs estimations are based on 'stationary' and 'direct-facing' subject measurements, which is not an ideal scenario for the complexity of sleep environment. This paper introduces novel real-time demodulation technique and respiratory & heart rates estimations algorithms applicable for embedded applications. This paper organized as follows: section 2 describes the non-contact bio-motion sensor that tracks a person's movement while sleeping. Based on these signals, respiratory and heart rates can then be estimated using novel real-time demodulation technique and estimations algorithms as explained in section 3 and 4. While section 5 report the outputs of the algorithms as compared with gold-standard Polysomnography (PSG) recordings from a set of twenty CHF patients who presented at a hospital sleep laboratory for evaluation of SDB. Finally, section 6 concludes the work presented in this paper.

2. Bio-motion Sensor and Patients Database

SleepMinder^{TM} (SM) is a ResMed patented novel sensor technology for contactless and convenient measurement of sleep and breathing in the home. SM is a dual pulse Doppler system designed to transmit two short pulses of radio frequency energy at 5.8 GHz and capable of measuring movements at distance between 0.5 – 3.0 meters, nominally. SM sensor also employed quadrature detection technique to overcome well known limitation in radio frequency sensing called the range-correlation effect, which leads to two estimates of the movements signals, called I and Q channels. In the case of two people lying on the bed, a combination of sophisticated sensor design and intelligent on-board signal processing results in measuring only the motions of the person nearest to the sensor. The outputs I and Q channels are internally filtered by active analogue low-pass filters at 1.6 Hz and sampled at 64 Hz with 12 bits, 0 – 3.2 Volts resolutions. The 64 Hz samples are then averaged over 4 samples, producing two 16 Hz channels and saved to the SM secure digital (SD) memory card in a proprietary binary format.

A database consists of twenty chronic heart failure (CHF) patients with New York Heart Association (NYHA) Heart Failure Classification Class II & III were selected for the study. The patients groups are of 1 female, 18 males and 1 undisclosed, who were sequentially admitted in the Royal Brompton Centre for Sleep, London, UK, for the diagnosis of sleep apnea, disordered sleep, or both. The patients mean age is 68.89 years, with mean body weight of 86.87 kg, mean BMI of 28.83 (obesity) and mean recorded sleep duration of 7.78 hours. The consented patients underwent full PSG analysis with manually scored by sleep experts. SM was installed in the sleep laboratory and its bio-motion signals were recorded simultaneously with the PSG signals. SM was placed facing the patient in line with chest at a distance of 0.5 meter and an elevation of 0.5 meter from the edge of the bed.

3. Real-Time Relative Demodulation Technique

This paper introduces novel real-time demodulation technique named 'Relative Demodulation'. The name is given as an attribute to the application of 'Relativity' concept in the demodulation of the subject's chest periodic motions. The novelty of this technique is that it pivoted from conventional displacement and/or phase-shift analysis to introduce derivatives analysis. This technique is real-time and provides the following advantages:

- DC offset, clutter and null-point automatic eliminations.
- Real-time approximations of the instantaneous derivatives of the subject's chest periodic motions.

- Real-time approximations & separation of the instantaneous subject's respiratory & heart periodic displacements.

The non-contact Doppler radar system baseband quadrature outputs I and Q channels generally expressed as:

$$I(t) = V_I + A_I \cos\left(\theta_0 + \frac{4\pi}{\lambda}(d_0 + x(t) + y(t)) + \Delta\phi(t)\right) \quad (V) \quad , \quad Q(t) = V_Q + A_Q \sin\left(\theta_0 + \frac{4\pi}{\lambda}(d_0 + x(t) + y(t)) + \Delta\phi(t)\right) \quad (V) \tag{1}$$

Where 'V_I' & 'V_Q' are the DC offsets and 'A_I' & 'A_Q' are the amplitude gain constants of the channels. 'θ_0' is the initial constant phase-shift of the system in radian. 'λ' is the wave length, which equal to the speed of light divided by the radar operating frequency. 'd_0' is the initial distant between the radar and subject's chest in meter. '$\Delta\phi$' is the phase noise of the system oscillation in radian. Let 'x(t)' be the function of respiratory that causes changes in the chest displacement in meter. Let 'y(t)' be the function of heart that causes changes in the chest displacement in meter. For physiological vital signs monitoring, the subject's chest distance usually within 0.5 – 3.0 meters, which make '$\Delta\phi(t)$' approaches zero, therefore, '$\Delta\phi(t)$' can be neglected.

In context of 'Relative Demodulation', I and Q channels from this point onwards are to be referred to as '*Observer I*' and '*Observer Q*'. The subject's chest periodic motions are to be referred to as '*Observation Target*'. The fundamental 'Relative Demodulation' concept for non-contact Doppler bio-motion system is as follows:

- Both '*Observer I*' and '*Observer Q*' are moving at the same speed, however, at different phases.
- The instantaneous derivatives of the '*Observer I*' and '*Observer Q*' are 'relative to' and 'impacted by' the instantaneous derivatives of the '*Observation Target*'.
- At any given point in time, both '*Observer I*' and '*Observer Q*' observed the same '*Observation Target*' instantaneous derivatives with respect to the other '*Observer*'.

The '*Observation Target*' instantaneous velocity as observed by '*Observer I*' with respect to '*Observer Q*' and '*Observer Q*' with respect to '*Observer I*' can be expressed as:

$$\frac{d}{dt}I(t) = -\frac{4\pi}{\lambda}\left(\frac{d}{dt}x(t) + \frac{d}{dt}y(t)\right)A_I \sin\left(\theta_0 + \frac{4\pi}{\lambda}(d_0 + x(t) + y(t))\right) \quad (V) \quad \rightarrow \quad x'(t) + y'(t) = -\frac{\lambda}{4\pi}\left(\frac{A_Q I'(t)}{A_I(Q(t) - V_Q)}\right) \quad (ms^{-1}) \tag{2}$$

$$\frac{d}{dt}Q(t) = \frac{4\pi}{\lambda}\left(\frac{d}{dt}x(t) + \frac{d}{dt}y(t)\right)A_Q \cos\left(\theta_0 + \frac{4\pi}{\lambda}(d_0 + x(t) + y(t))\right) \quad (V) \quad \rightarrow \quad x'(t) + y'(t) = \frac{\lambda}{4\pi}\left(\frac{A_I Q'(t)}{A_Q(I(t) - V_I)}\right) \quad (ms^{-1}) \tag{3}$$

As shown in (2) and (3), both '*Observer I*' and '*Observer Q*' observed the same '*Observation Target*' instantaneous velocity. The null-points can be eliminated by averaging the observed instantaneous velocity of both '*Observer I*' and '*Observer Q*'. The resultant '*Observation Target*' instantaneous velocity can be expressed as:

$$\therefore \quad v(t) = x'(t) + y'(t) = \frac{\lambda}{8\pi}\left(\frac{kQ'(t)}{(I(t) - V_I)} - \frac{I'(t)}{k(Q(t) - V_Q)}\right) \quad (ms^{-1}) \quad where: \quad k = \frac{A_I}{A_Q} \tag{4}$$

As shown in (4) the DC offset of the channels are eliminated by both the subtraction of 'V_I' & 'V_Q' and the first derivative. The constant phase-shift and clutter are also eliminated by the first derivative. Let '$h_r(t)$' be the respiratory band-pass filter (RBPF). The RBPF filter type, gain and frequency bandwidth will be discussed in section 4. The '*Observation Target*' instantaneous respiratory velocity and displacement can be expressed as:

$$x'(t) = h_r(t) * v(t) \quad (ms^{-1}) \quad \Leftrightarrow \quad x(t) = \int (h_r(t) * v(t))dt \quad (m) \tag{5}$$

We learnt from pathophysiology and anatomy that respiration requires inspiration and expiration efforts, which contains both velocity and acceleration. The heart systole (contraction) and diastole (relaxation) also contains both

velocity and acceleration. The chest periodic displacements are caused by the velocity and acceleration of the inspiration-expiration and systole-diastole cycles in combination. We also learnt from physics that the third derivative, often referred to as 'jerk', describes the changes of acceleration. Therefore, to describe the changes that the heart acceleration acted on the respiration acceleration, the resultant '*Observation Target*' instantaneous jerk has to be derived. The resultant '*Observation Target*' instantaneous jerk can be expressed as:

$$\therefore \quad j(t) = x'''(t) + y'''(t) = \frac{\lambda}{8\pi}\left(\frac{kQ'(t)}{(I(t)-V_I)} - \frac{I'(t)}{k(Q(t)-V_Q)}\right)'' \quad \left(ms^{-3}\right) \quad where: \quad k = \frac{A_I}{A_Q} \tag{6}$$

Let '$h_h(t)$' be the heart band-pass filter (HBPF). The HBPF filter type, gain and frequency bandwidth will be discussed in section 4. The '*Observation Target*' instantaneous heart jerk and displacement can be expressed as:

$$y'''(t) = (h_h(t) * j(t)) \quad \left(ms^{-3}\right) \quad \Leftrightarrow \quad y(t) = \iiint (h_h(t) * j(t))dt \quad (m) \tag{7}$$

Backwards-difference and Trapezoidal integration with unit spacing numerical approximations has been selected for its simplicity in implementation to discretise the real-time 'Relative Demodulation' derivatives and displacements. The discretised 'Relative Demodulation' equations with 'f_s' as the sample rate in Hertz are as follows:

$$\therefore \quad v[n] = x'[n] + y'[n] = \frac{\lambda}{8\pi} f_s \left[\frac{k[Q[n]-Q[n-1]]}{[I[n]-V_I]} - \frac{[I[n]-I[n-1]]}{k[Q[n]-V_Q]}\right] \quad \left(ms^{-1}\right) \quad where: \quad k = \frac{A_I}{A_Q} \tag{8}$$

$$x'[n] = h_r[n] * v[n] \quad \left(ms^{-1}\right) \quad \Leftrightarrow \quad x[n] = x[n-1] + \left[\frac{x'[n] + x'[n-1]}{2f_s}\right] \quad (m) \tag{9}$$

$$\therefore \quad j[n] = x'''[n] + y'''[n] = f_s^2[v[n] - 2v[n-1] + v[n-2]] \quad \left(ms^{-3}\right) \tag{10}$$

$$\begin{aligned} y'''[n] = h_h[n] * j[n] \quad \left(ms^{-3}\right) \quad \Leftrightarrow \quad & a_h[n] = a_h[n-1] + \left[\frac{y'''[n] + y'''[n-1]}{2f_s}\right] \quad \left(ms^{-2}\right) \\ & v_h[n] = v_h[n-1] + \left[\frac{a_h[n] + a_h[n-1]}{2f_s}\right] \quad \left(ms^{-1}\right) \\ \therefore \quad & y[n] = y[n-1] + \left[\frac{v_h[n] + v_h[n-1]}{2f_s}\right] \quad (m) \end{aligned} \tag{11}$$

4. Respiratory and Heart Rates Estimations Algorithms

This paper also introduces novel real-time inspiration & expiration detection, systole & diastole detection and respiratory & heart rates estimations algorithms, pioneering the estimations of respiratory and heart rates for chronic heart failure (CHF) patients in the complexity of sleep environment. The novelty of these algorithms is that it is real-time, fast, accurate, low computational and applicable for embedded applications.

As indicated in section 2, the SleepMinder™ analogue-to-digital converter (ADC) voltage resolution is 0 – 3.2 Volts. The voltage mean value, which is the reference DC offset, is equal to 1.6 V. Therefore, V_I & V_Q are approximately equal to 1.6 V. According to the undisclosed SleepMinder™ technical specifications, channels I and Q amplitude gain constants are approximately equal and are typically 15 – 20 dB. Therefore, the amplitude gain constants A_I & A_Q are approximately equal and their ratio 'k' is also approximately equal to 1.0.

Butterworth band-pass filter has been chosen to implement both respiratory band-pass filter (RBPF) and heart band-pass filter (HBPF). The reason for choosing such type of filter is that the frequency response of Butterworth filter is maximally flat (i.e. has no ripples) in the pass-band and rolls off towards zero in the stop-band. In addition,

the implementation of Butterworth filter is much simpler and performs much faster as compared to other FIR filters, which is more applicable for embedded applications. The selected frequency bandwidth for RBPF is 0.2 – 0.5 Hz corresponds to 12 – 30 breaths per minute. The selected frequency bandwidth for HBPF is 0.7 – 1.6 Hz corresponds to 42 – 96 beats per minute. The order of the Butterworth band-pass filter has been chosen to be at 6^{th} order with unity gain.

The key to inspiration & expiration detection algorithm relied on the discretised '*Observation Target*' instantaneous respiratory velocity as specified in (9). The detection rules for inspiration 'i[n]' and expiration 'e[n]' can be expressed as:

$$i[n]=\begin{cases}1, & x'[n]\le 0 \wedge x'[n-1]\succ 0 \wedge R1 \wedge R2\\ 0, & otherwise\end{cases}\quad,\quad e[n]=\begin{cases}1, & x'[n]\ge 0 \wedge x'[n-1]\prec 0 \wedge R1 \wedge R2\\ 0, & otherwise\end{cases} \tag{12}$$

- R1: The current detected inspiration/expiration index with value equal 1, subtracts the previous detected inspiration/expiration index with value equal 1, have to be greater or equal to '$2f_s$', where 'f_s' is the ADC sample rate in Hertz. This allows up to a maximum of 0.5 Hz to be detected, any higher frequency will be ignored.
- R2: The current detected inspiration/expiration index with value equal 1, subtracts the previous detected expiration/inspiration index with value equal 1, have to be greater or equal to 'f_s'.

The key to systole & diastole detection algorithm relied on the discretised '*Observation Target*' instantaneous heart jerk as specified in (11). The detection rules for systole 's[n]' and diastole 'd[n]' can be expressed as:

$$s[n]=\begin{cases}1, & y'''[n]\le 0 \wedge y'''[n-1]\succ 0 \wedge H1 \wedge H2\\ 0, & otherwise\end{cases}\quad,\quad d[n]=\begin{cases}1, & y'''[n]\ge 0 \wedge y'''[n-1]\prec 0 \wedge H1 \wedge H2\\ 0, & otherwise\end{cases} \tag{13}$$

- H1: The current detected systole/diastole index with value equal 1, subtracts the previous detected systole/diastole index with value equal 1, have to be greater or equal to '$0.5f_s$', where 'f_s' is the ADC sample rate in Hertz. This allows up to a maximum of 2 Hz to be detected, any higher frequency will be ignored.
- H2: The current detected systole/diastole index with value equal 1, subtracts the previous detected diastole/systole index with value equal 1, have to be greater or equal to '$0.25f_s$'.

The respiratory rate can be estimated from the averaged sum of the detected inspiration and expiration cycles per selected window-width. The heart rate can be estimated from the averaged sum of the detected systole and diastole cycles per selected window-width. For this research purpose, a fixed window-width of 60 seconds (2 epochs) and a sliding window-width of 30 seconds (1 epoch) are employed.

5. Results and Discussions

A patient (out of 20) was selected as an example to demonstrate the accuracy of the real-time 'Relative Demodulation' technique and estimations algorithms and is shown in "Fig. 2". "Fig. 2 (a)" top and bottom left-side graphs with a data segment of 60 seconds shows that the respiratory displacement accurately demodulated as compared to the PSG RIP Thorax respiratory signal. The inspirations and expirations have also been accurately detected. "Fig. 2 (a)" top and bottom right-side graphs with a data segment of 10 seconds shows that the heart displacement accurately demodulated as compared to the PSG ECG signal. The systoles (troughs) and diastoles (peaks) have also been accurately detected. "Fig. 2 (b)" shows that the SM estimated respiratory and heart rates track along exceptionally well with the estimated RIP Thorax respiratory and ECG heart rates for the entire duration of the sleep recording of 6.39 hours. The differences in the x-axis for all graphs are due to the resampled PSG data.

The performance measure was also obtained for all twenty chronic heart failure (CHF) patients and is shown in "Fig. 3". Across all twenty CHF patients' recordings, the respiratory rate estimation median accuracy achieved 91.52% with median error of ±1.31 breaths/minute. The heart rate estimation median accuracy achieved 91.29% with median error of ±6.16 beats/minute.

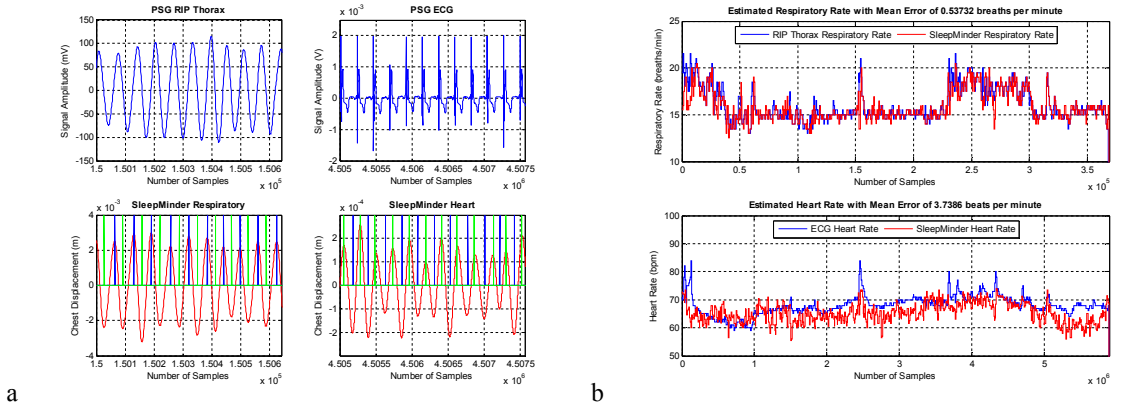

a b

Fig. 2. (a) SleepMinder™ demodulated respiratory & heart displacements; (b) SleepMinder™ vs. PSG estimated respiratory and heart rates.

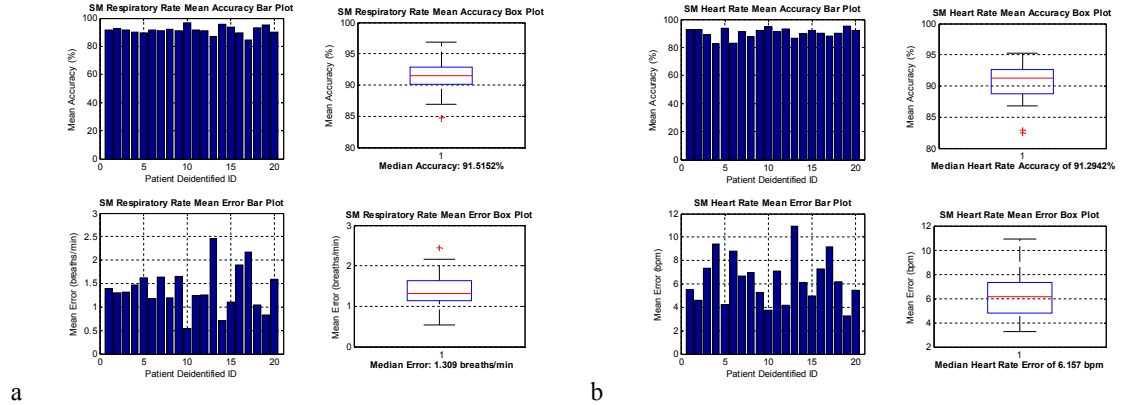

a b

Fig. 3. (a) SleepMinder™ estimated respiratory rate mean accuracy and error; (b) SleepMinder™ estimated heart rate mean accuracy and error.

6. Conclusion

The novel real-time ‘Relative Demodulation’ technique and respiratory & heart rates estimations algorithms have been demonstrated with good accuracy for twenty chronic heart failure (CHF) patients in the complexity of sleep environment. A potential application would be home continuous sleep and circadian rhythm monitoring.

Acknowledgements

The authors would like to acknowledge the support of ResMed in providing the patented non-contact bio-motion sensor and patients’ database for this study.

References

1. Peppard, P. E., Young, T., Barnet, J. H., Palta, M., Hagen, E. W., and Hla, K. M., *Increased Prevalence of Sleep-Disordered Breathing in Adults.* American Journal of Epidemiology, 2013. **177**(9): p. 1006-1014.
2. Marshall, N. S., Wong, K. K. H., Cullen, S. R. J., Knuiman, M. W., and Grunstein, R. R., *Sleep Apnea and 20-Year Follow-Up for All-Cause Mortality, Stroke, and Cancer Incidence and Mortality in the Busselton Health Study Cohort.* Journal of Clinical Sleep Medicine, 2014. **10**(4): p. 355-362.